

**Planar Dy<sub>3</sub>+Dy<sub>3</sub> clusters: Design, structures and axial ligands perturbed magnetic dynamics**

Journal:	<i>Dalton Transactions</i>
Manuscript ID	DT-COM-10-2015-003931
Article Type:	Communication
Date Submitted by the Author:	08-Oct-2015
Complete List of Authors:	Li, Xiao-Lei; Changchun Institute of Applied Chemistry, Li, Han; Nankai University, Department of Chemistry Chen, Diming; Nankai University, Department of Chemistry Wang, Chao; Nankai University, Department of Chemistry Wu, Jianfeng; Changchun Institute of Applied Chemistry, State Key Laboratory of Rare Earth Resource Utilization Cheng, Peng; Nankai University, Department of Chemistry Tang, Jinkui; Changchun Institute of Applied Chemistry, State Key Laboratory of Rare Earth Resource Utilization



Journal Name

COMMUNICATION

## Planar Dy<sub>3</sub>+Dy<sub>3</sub> clusters: Design, structures and axial ligands perturbed magnetic dynamics

Received 00th January 20xx,  
Accepted 00th January 20xx

Xiao-Lei Li,<sup>ab</sup> Han Li,<sup>a</sup> Di-Ming Chen,<sup>a</sup> Chao Wang,<sup>b</sup> Jianfeng Wu,<sup>b</sup> Jinkui Tang<sup>\*b</sup> and Peng Cheng<sup>a</sup>

DOI: 10.1039/x0xx00000x

www.rsc.org/

**Two unique Dy<sub>6</sub> complexes with fascinating Dy<sub>3</sub>+Dy<sub>3</sub> structures were assembled, showing single-molecule magnetic behavior with high energy barriers of 116 and 181 K for Dy<sub>6</sub>-NO<sub>3</sub> and Dy<sub>6</sub>-SCN.**

Lanthanide single-molecule magnets (SMMs), whose relaxation and quantum tunneling of the magnetization are molecule-based, have been receiving much attention with the collective aim of practical applications in high density information storage,<sup>1</sup> molecular spintronic,<sup>2</sup> and quantum processing<sup>3</sup> at a molecular level since the slow relaxation of the magnetization at liquid nitrogen temperature could be observed in the so-called double decker phthalocyanines, (Bu<sub>4</sub>N)[Tb(Pc)<sub>2</sub>].<sup>4</sup> Such molecules with strong magnetic anisotropy could, at liquid-helium temperatures, relax their magnetization slowly and retain magnetization for long periods of time in the absence of an external magnetic field.<sup>5</sup> After that, and especially in the last five years, considerable attention has therefore focused on coordination compounds of the f-elements, particularly those of the lanthanides, have accounted for some of the most eye-catching recent advances in molecular magnetism.<sup>6</sup>

The design of new single-molecule magnets (SMMs) with appealing topologies and fascinating magnetic behavior remains an attractive challenge. In 2006, Powell's group reported a paradigm Dy<sub>3</sub> complex with unusual slow relaxation of the magnetization observed in spite of an almost non-magnetic ground state.<sup>7</sup> Since then, polynuclear Dy<sup>III</sup> SMMs have attracted much interest besides the well-established monometallic systems.<sup>8</sup> Further investigations toward utilizing this highly anisotropic Dy<sub>3</sub> triangle as building blocks to create larger SMMs were stimulated by its unprecedented magnetic

properties. Indeed, with the aim of creating new lanthanide SMMs and also to further probe the unique properties of such systems, the opening up and linkage of such highly anisotropic dysprosium triangles in different forms have become a hot topic.<sup>9</sup> Our group has long been aiming to focus our attention on using Dy<sub>3</sub> triangles as building blocks to create larger SMMs through modifying the capping as well as surrounding ligands.<sup>9b,10</sup> Notably, the coupling of two Dy<sub>3</sub> triangles via a μ<sub>4</sub>-O<sup>2-</sup> ion has been found to enhance the toroidal moments.<sup>7,9c</sup> As our continuing studies on triangular Dy<sub>3</sub>-based triangles system, herein, we report the syntheses, structural and magnetic investigation of two novel Dy<sub>6</sub> clusters with formula [Dy<sub>6</sub>L<sub>2</sub>(μ<sub>3</sub>-OH)<sub>4</sub>(μ<sub>2</sub>-OH)<sub>2</sub>(SCN)<sub>8</sub>(H<sub>2</sub>O)<sub>4</sub>]·6CH<sub>3</sub>CN·2CH<sub>3</sub>OH·H<sub>2</sub>O (**Dy<sub>6</sub>-SCN**) and [Dy<sub>6</sub>L<sub>2</sub>(μ<sub>3</sub>-OH)<sub>4</sub>(μ<sub>2</sub>-OH)<sub>2</sub>(NO<sub>3</sub>)<sub>6</sub>(H<sub>2</sub>O)<sub>6</sub>]·2NO<sub>3</sub>·10H<sub>2</sub>O (**Dy<sub>6</sub>-NO<sub>3</sub>**) in which two discrete Dy<sub>3</sub> triangles are aggregated in a novel planar Dy<sub>3</sub>+Dy<sub>3</sub> fashion encapsulated by multidentate Schiff-base ligand. These clusters provide a unique opportunity to understand the interplay between Dy<sub>3</sub> triangles and to probe the relaxation dynamics influenced by the axial ligands in each triangle. Magnetic analysis reveals that these compounds display similar dc magnetic behavior but dissimilar dynamic magnetic behaviour with a relatively high energy barrier for **Dy<sub>6</sub>-SCN** among the reported polynuclear lanthanide SMMs, reaching 181 K. The dissimilar dynamic magnetic behavior originates from the structural differences in light of the coordination environment of Dy<sup>III</sup> ions, which alter the local tensor of anisotropy and crystal-field splitting on each Dy site.

The reactions of H<sub>2</sub>L (Scheme S1) and Dy(NO<sub>3</sub>)<sub>3</sub>·6H<sub>2</sub>O or Dy(SCN)<sub>3</sub>·6H<sub>2</sub>O in the presence of triethylamine produce yellow crystals of **Dy<sub>6</sub>-SCN** and **Dy<sub>6</sub>-NO<sub>3</sub>**, respectively. The molecular structures established by single crystal X-ray diffraction are depicted in Fig.1, top and Fig. S1 (ESI<sup>†</sup>).

The structure of complex **Dy<sub>6</sub>-SCN** contains a hexanuclear Dy<sub>6</sub> core and can be regarded as the linkup of two [Dy<sub>3</sub>(μ<sub>3</sub>-O)<sub>2</sub>(μ<sub>2</sub>-O)<sub>3</sub>] (Fig. 1, bottom left) triangular units in an edge-to-edge arrangement encapsulated by two deprotonated L<sup>2-</sup> ligands. Each triangular unit is capped by two μ<sub>3</sub>-hydroxo atoms, in which the vertices of the triangles are linked via two bridging phenol O (O2, O4) atoms of two L<sup>2-</sup> ligands and one

<sup>a</sup> Department of Chemistry, Key Laboratory of Advanced Energy Materials Chemistry (MOE), and Innovation Center of Chemical Science and Engineering (Tianjin), Nankai University, Tianjin 300071, P. R. China

<sup>b</sup> State Key Laboratory of Rare Earth Resource Utilization, Changchun Institute of Applied Chemistry, Chinese Academy of Sciences, Changchun 130022, P. R. China. Fax: +86 431 85262878; E-mail: tang@ciac.ac.cn

<sup>†</sup> Electronic supplementary information (ESI) available: Experimental details, structural figures, crystallographic data, magnetic and spectroscopic characterization. CCDC 1419275 and 1419276. For ESI and crystallographic data in CIF or other electronic format see DOI: 10.1039/x0xx00000x

bridging hydroxo atom (O3). Within the triangle, Dy1 is further coordinated by two methoxy groups; Dy2 and Dy3 are each coordinated by one pyrimidine N and one imine N. In axial positions on opposite sides of the triangle, the remaining coordination sites are completed by two  $\text{SCN}^-$  anions for Dy1; one water molecule and one  $\text{SCN}^-$  anion for Dy2/Dy3. Accordingly, all of  $\text{Dy}^{\text{III}}$  ions are eight-coordinate but with different coordination geometries; Dy1 possesses a slightly distorted square-antiprismatic geometry, whereas Dy2 and Dy3 possess distorted dodecahedral geometry (Fig. 1, bottom right and Table S1).

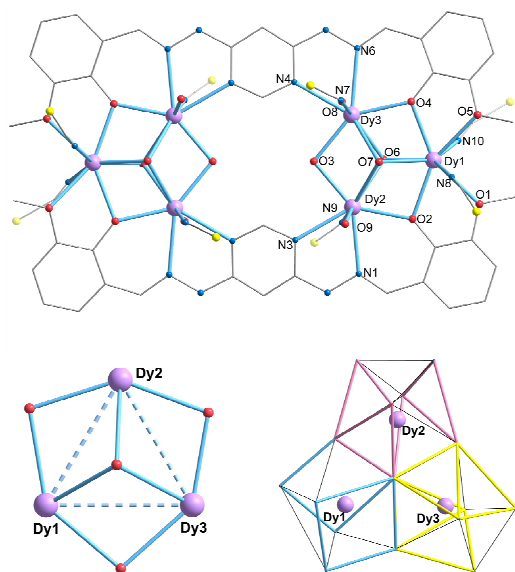


**Fig. 1** (top) Partially labeled  $\text{Dy}_6$  structure of complex  $\text{Dy}_6\text{-SCN}$  with the central core highlighted by thick bonds and solvent molecules are omitted for clarity. Color scheme: pink, Dy; red, O; blue, N; yellow, S. (bottom left) Overall central core for  $\text{Dy}_6\text{-SCN}$ . (bottom right) Coordination polyhedra observed in  $\text{Dy}_6\text{-SCN}$ : square-antiprismatic environment for Dy1 and triangular dodecahedron geometries for Dy2/Dy3.

The structure of  $\text{Dy}_6\text{-NO}_3$  is actually isomorphous to  $\text{Dy}_6\text{-SCN}$  and has a similar framework with  $\text{Dy}_6\text{-SCN}$ , except that two  $\text{H}_2\text{O}$  molecules coordinate to Dy1; one chelating  $\text{NO}_3^-$  and one  $\text{H}_2\text{O}$  molecule to Dy2; one chelating  $\text{NO}_3^-$  and one monodentate nitrate anions to Dy3 in axial positions on opposite sides of the triangle (Fig. S1, ESI<sup>†</sup>). Accordingly, because of the chelating  $\text{NO}_3^-$  for Dy2 and Dy3 so both of them possess a distorted monocapped square-antiprismatic geometry, whereas Dy1 possesses a slightly distorted square-antiprismatic geometry (Table S2).

Both  $\text{Dy}_3$  triangles within two complexes are close to equilateral triangle and the average Dy...Dy distances within the triangles are 3.526(3) and 3.518 Å for  $\text{Dy}_6\text{-SCN}$  and  $\text{Dy}_6\text{-NO}_3$ , respectively. The angles within the triangles of two complexes are also very close to 60°. The two planes derived from the two  $\text{Dy}_3$  triangles are parallel to each other in  $\text{Dy}_6\text{-NO}_3$  and nearly coplanar with distance of 0.236(1) Å between two  $\text{Dy}_3$  planes. In contrast, there is a small dihedral angle of 5.135° between the two planes in  $\text{Dy}_6\text{-SCN}$  (Table S4, ESI<sup>†</sup>).

The direct current magnetic properties of  $\text{Dy}_6\text{-SCN}$  and  $\text{Dy}_6\text{-NO}_3$  were measured under a 1000 Oe dc field in the temperature range 2–300 K. As shown in Fig. 2, the dc magnetic properties of these two complexes are nearly identical to each other. The room-temperature  $\chi_M T$  values of 78.3 and 80.9  $\text{cm}^3\text{mol}^{-1}\text{K}$  for  $\text{Dy}_6\text{-SCN}$  and  $\text{Dy}_6\text{-NO}_3$  are slightly lower than the value expected ( $^6\text{H}_{15/2}$ ,  $S = 5/2$ ,  $L = 5$ ,  $J = 15/2$ ,  $g = 4/3$ ) for six magnetically isolated  $\text{Dy}^{\text{III}}$  ions. At lower temperatures, the  $\chi_M T$  values decrease slowly down to approximately 25 K then rapidly down to 2 K reaching values of 57.1 and 53.4  $\text{cm}^3\text{mol}^{-1}\text{K}$  for  $\text{Dy}_6\text{-SCN}$  and  $\text{Dy}_6\text{-NO}_3$ , respectively. This behaviour is therefore dissimilar to that of the original  $\text{Dy}_3$  triangles with an almost non-magnetic ground state. The decline of  $\chi_M T$  with lowering temperature is mainly due to the thermal depopulation of the excited states of the  $\text{Dy}^{\text{III}}$  ions. Moreover, weak antiferromagnetic coupling between  $\text{Dy}^{\text{III}}$  centers can also contribute to this behaviour but cannot be easily quantified due to the orbital angular momentum of the  $\text{Ln}^{\text{III}}$  ions.

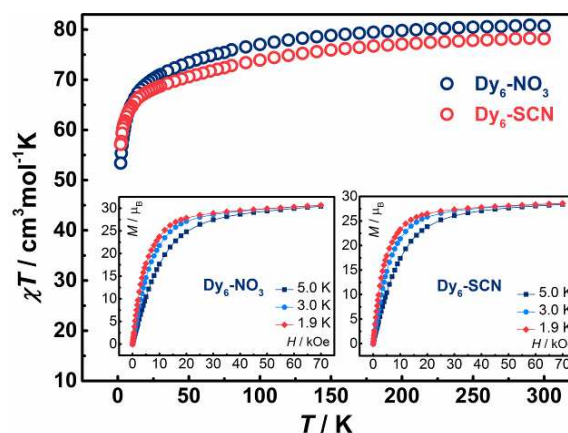


**Fig. 2** Temperature dependence of the  $\chi_M T$  product for  $\text{Dy}_6\text{-SCN}$  and  $\text{Dy}_6\text{-NO}_3$ . Inset: Field dependence of the magnetization for  $\text{Dy}_6\text{-SCN}$  and  $\text{Dy}_6\text{-NO}_3$ , the solid lines are guides to the eye.

Magnetization ( $M$ ) data for  $\text{Dy}_6\text{-SCN}$  and  $\text{Dy}_6\text{-NO}_3$  were collected in the 0–70 kOe field range below 5 K.  $M$  increase smoothly with increasing applied dc field without saturation even at 1.9 K and under 7 T (Fig. 2 inset and Fig. S3, ESI<sup>†</sup>). The  $M$  vs.  $H/T$  plots (Fig. S2, ESI<sup>†</sup>), do not superimpose in a master-curve and the high field non-saturation indicates the presence of significant magnetic anisotropy and/or low-lying excited states in these two complexes.

In view of the interesting magnetic behavior of the reported  $\text{Dy}_3$  and coupling  $\text{Dy}_3$  triangles,<sup>7, 10e</sup> alternating current (ac) susceptibility measurements were carried out for  $\text{Dy}_6\text{-SCN}$  and  $\text{Dy}_6\text{-NO}_3$  in the frequency range 1–1500 Hz under a zero-dc field to investigate the dynamics of the magnetization. As shown in Fig. 3, it is very striking that the presence of a series of frequency-dependent peaks in a relatively wide temperature range reveal slow magnetic relaxation behavior typical of SMMs for both complexes. For  $\text{Dy}_6\text{-SCN}$ , it is worth noting that a second tail of peak in  $\chi''$  at higher frequencies appears besides the first peak at much lower frequencies

between 1.9–9 K (Fig. S5), implying the possible occurrence of two relaxation processes. However, above 9 K (Fig. S6), only a single peak can be observed at higher frequencies, indicating the evolution from fast relaxation (FR) to slow relaxation (SR) within the frequency range of the test with increasing temperature. The Cole–Cole plots showing two well separated relaxation phases below 10 K (Figs. S7; S8, ESI†) and an asymmetric semicircle above 10 K (Fig. S9, ESI†), further indicate the evolution from FR to SR as the temperature is raised. The Cole–Cole plots for **Dy<sub>6</sub>–SCN** in the temperature range of 1.9–9 K exhibited two separate relaxation processes, which can be nicely fitted to the sum of two modified Debye functions (eq. 1),<sup>11</sup> according to two relaxation processes with  $\alpha_1$  parameters larger than 0.48, suggesting a wide distribution of relaxation time constants for SR. In contrast, the small parameters  $\alpha_2$  indicate a small distribution of relaxation times for FR. (Table S5, ESI†). Furthermore, the plots with a nearly semicircle shape from 10 to 22 K can be fitted well to the generalized Debye function gives small values of  $\alpha$  ( $\alpha < 0.25$ ) suggests a narrow distribution of relaxation time constants (Table S6, ESI†).

$$\chi_{AC}(\omega) = \chi_{S, \text{tot}} + \frac{\Delta\chi_1}{1 + (i\omega\tau_1)^{(1-\alpha_1)}} + \frac{\Delta\chi_2}{1 + (i\omega\tau_2)^{(1-\alpha_2)}} \quad (1)$$

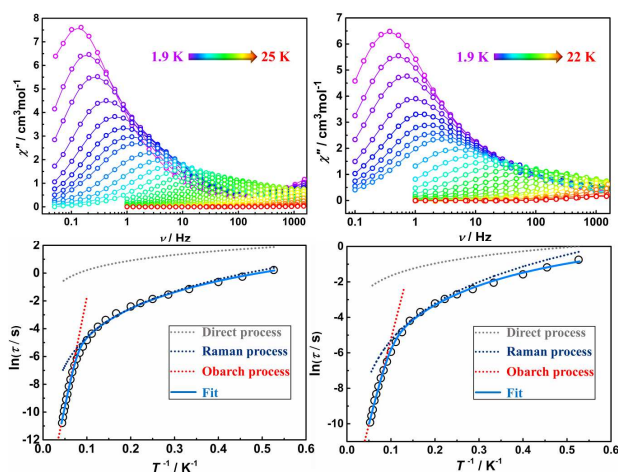


**Fig. 3** Frequency dependence of the out-of-phase ac susceptibility under zero applied dc field for **Dy<sub>6</sub>–SCN** (top left) and **Dy<sub>6</sub>–NO<sub>3</sub>** (top right), the solid lines are guides to the eye. Bottom: Fitting of Arrhenius plot based on eq. 2 and relaxation times obtained by simultaneous fitting of  $\chi'$  and  $\chi''$  vs  $\nu$  plots for **Dy<sub>6</sub>–SCN** (bottom left) and **Dy<sub>6</sub>–NO<sub>3</sub>** (bottom right).

The relaxation times were obtained from fitting the frequency-dependent magnetic susceptibility data between 1.9 and 24 K using the generalized Debye model and plotted vs.  $1/T$  to give an Arrhenius plot. (Fig. 3, bottom left) Arrhenius plot does exhibit obvious curvature, indicates a combination of the relaxation pathways has to be taken into account so as to understand the relaxation behavior. It is worth noting that the relaxation times are always temperature-dependent in the whole temperature regime (Fig. 3, top left), which suggests the relaxation process is dominated by Orbach mechanism at the high temperature and Raman mechanism at the low

temperature rather than Direct mechanism which is expected to be controlled by quantum tunneling effects (direct relaxation process), even the temperature down to 1.9 K. The linear fit of the  $\ln(\tau)$  versus  $\ln(T)$  plot giving an  $n$  value of 2.8, indicates further that the system relaxes mainly via Orbach and Raman processes instead of Direct process (Fig. S13, ESI†). Data in the entire 1.9–25 K temperature range were analyzed by the following equation:<sup>12</sup> two modified Debye functions (eq 1),<sup>11</sup>

$$\ln \tau = -\ln[AT + B + CT^n + \tau_0^{-1} \exp(-U_{\text{eff}}/k_B T)] \quad (2)$$

where  $AT+B$ ,  $CT^n$ , and  $\tau_0^{-1} \exp(U_{\text{eff}}/k_B T)$  represent direct, Raman, and Orbach relaxation processes, respectively. Firstly, the energy barrier is obtained by modeling the behavior with the Arrhenius law ( $\tau = \tau_0 \exp(U_{\text{eff}}/k_B T)$ ) above 15 K (15–25 K; red dotted line, Fig. 3 bottom left) to give the  $U_{\text{eff}}$  of 181(6) K with pre-exponential factor  $\tau_0$  of  $8.1(2) \times 10^{-9}$  s. Accordingly,  $U_{\text{eff}}$  and  $\tau_0$  were fixed to above values, after that the value of  $B$  parameter was fixed to zero based on the linear fit to the plot  $\ln \tau$  versus  $\ln T$  in the range of 1.9–5 K. With these restraints, assuming  $n = 3, 5, 7$ , or 9 and letting the  $A$  and  $C$  parameters to vary freely, the plot in the temperature range 1.9–25 K was fitted successfully using eq. 2. The best fit was obtained for  $n = 3.65$  and  $A = 0.3779 \text{ s}^{-1} \text{ K}^{-3.65}$ ,  $C = 0.02734$  (Fig. 3 bottom left). The small  $A$  and  $C$  values further indicate the relaxation process is dominated by Orbach mechanism at the high temperature and Raman mechanism at the low temperature where the curvature of the Arrhenius plot is the transition from Raman to Orbach relaxation.

Now let's discuss the ac magnetic property of the complex **Dy<sub>6</sub>–NO<sub>3</sub>**. Significant slow relaxation of magnetization is also observed in ac susceptibilities below 22 K under zero dc field (Fig. 3 top right). In contrast to **Dy<sub>6</sub>–SCN**, only a single broad shoulder can be observed within the whole frequency range with increasing temperature for **Dy<sub>6</sub>–NO<sub>3</sub>**, which suggests the multiple relaxation processes. Accordingly, to quantify this effect, fitting the data to a generalized Debye equation to extract relaxation times, and an Arrhenius plot was constructed to study the temperature dependence of the magnetic relaxation (Fig. 3 bottom right). As expected for a single-molecule magnet, the relaxation times exhibit an exponential dependence on temperature, and in the high-temperature regime, the relaxation process of **Dy<sub>6</sub>–NO<sub>3</sub>** follows an Arrhenius law with an effective energy barrier  $U_{\text{eff}} = 116$  K and a pre-exponential factor  $\tau_0 = 1.11 \times 10^{-7}$  s. In view of the similar relaxation processes with **Dy<sub>6</sub>–SCN**, the plot of  $\ln(\tau)$  versus  $\ln(T)$  was also analyzed by eq. 2 in the entire temperature range 1.9–22 K. The plot was fitted successfully using eq. 2 with the fitting parameters  $n = 3.24$  and  $A = 0.70649 \text{ s}^{-1} \text{ K}^{-3.24}$ ,  $C = 0.13323$  (Fig. 3 bottom right).

The Cole–Cole plots (Fig. S10–S12) in the temperature range 1.9–22 K were fitted to the generalized Debye model to further investigate the distribution of the relaxation processes. Attempted fits of the data gave large  $\alpha$  parameters ( $\alpha < 0.43$ ) indicating a wide distribution of relaxation time constants (Table S7, ESI†).

Generally, for pure 4f-SMMs, the slow magnetic relaxation mainly derived from single-ion anisotropy, which is extremely sensitive to tiny distortion of the coordination geometry. Here, both Dy<sub>3</sub>+Dy<sub>3</sub> cores of Dy<sub>6</sub>-SCN and Dy<sub>6</sub>-NO<sub>3</sub> are encapsulated by two symmetrical Schiff base ligands with similar equatorial coordination environment. However, auxiliary ligands in axial direction are remarkably different (see above). Hence, such structural differences result from the change of coordination environments in axial direction probably affect the local tensor of anisotropy and further affect the directions of the easy axes on each dysprosium site through the local ligand-fields of the terminal anions, thus causing distinct dynamic behaviour.<sup>9b, 10b</sup>

In summary, two novel Dy<sub>6</sub> complexes based on triangular unit have been successfully designed using a symmetrical Schiff base ligand H<sub>2</sub>L. Complexes Dy<sub>6</sub>-SCN and Dy<sub>6</sub>-NO<sub>3</sub> show fascinating Dy<sub>3</sub>+Dy<sub>3</sub> structures and prominent SMM behavior with a larger energy barrier for Dy<sub>6</sub>-SCN, reaching 181 K. Interestingly, both complexes display similar dc magnetic behaviors, however, different magnetic dynamic behavior is observed. The Dy<sub>3</sub>+Dy<sub>3</sub> cores are encapsulated inside the coordination pockets of two ligands, but with different axial coordination anions. Accordingly, the structural difference results in different coordination geometries for Dy<sub>2</sub> and Dy<sub>3</sub> in these two complexes, thus affecting the directions of the easy axes on each dysprosium site through the local ligand-fields of the terminal anions, which influences the dynamics of magnetic relaxation. These results offer a promising strategy into the fine-tuning of the magnetic properties of SMMs by slightly modifying the coordination geometry through introducing different auxiliary ligands in axial positions. The synthesis and investigation of new clusters incorporating triangular Dy<sub>3</sub> unit are in progress to explore the effect of auxiliary ligands and the arrangement of Dy<sub>3</sub> unit on the toroidal magnetic moments.

We thank the National Natural Science Foundation of China (Grants 21371166, 21331003, and 21221061) for financial support.

## Notes and references

- 1 R. Sessoli, D. Gatteschi, A. Caneschi and M. A. Novak, *Nature*, 1993, **365**, 141.
- 2 (a) D. Gatteschi, R. Sessoli and R. Villain, *Molecular Nanomagnets*, Oxford University Press, New York, 2006; (b) L. Bogani and W. Wernsdorfer, *Nat. Mater.*, 2008, **7**, 179; (c) S. Sanvito, *Chem. Soc. Rev.*, 2011, **40**, 3336.
- 3 (a) D. Gatteschi and R. Sessoli, *Angew. Chem. Int. Ed.*, 2003, **42**, 268; (b) M. N. Leuenberger and D. Loss, *Nature*, 2001, **410**, 789.
- 4 N. Ishikawa, M. Sugita, T. Ishikawa, S. Koshihara and Y. Kaizu, *J. Am. Chem. Soc.*, 2003, **125**, 8694.
- 5 (a) R. Sessoli, H. L. Tsai, A. R. Schake, S. Wang, J. B. Vincent, K. Folting, D. Gatteschi, G. Christou and D. N. Hendrickson, *J. Am. Chem. Soc.*, 1993, **115**, 1804; (b) L. Sorace, C. Benelli and D. Gatteschi, *Chem. Soc. Rev.*, 2011, **40**, 3092.
- 6 (a) P. Zhang, L. Zhang, C. Wang, S. Xue, S.-Y. Lin and J. Tang, *J. Am. Chem. Soc.*, 2014, **136**, 4484; (b) E. Moreno Pineda, N. F. Chilton, R. Marx, M. Dörfel, D. O. Sells, P. Neugebauer, S.-D. Jiang, D. Collison, J. van Slageren, E. J. L. McInnes and R. E. P. Winpenny, *Nat. Commun.*, 2014, **5**, 5243; (c) J. D. Rinehart, M. Fang, W. J. Evans and J. R. Long, *Nat. Chem.*, 2011, **3**, 538; (d) J. Tang and P. Zhang, *Lanthanides Single Molecule Magnets*, Springer Heidelberg, 2015; (e) J. J. Le Roy, M. Jeletic, S. I. Gorelsky, I. Korobkov, L. Ungur, L. F. Chibotaru and M. Murugesu, *J. Am. Chem. Soc.*, 2013, **135**, 3502; (f) Y.-N. Guo, G.-F. Xu, W. Wernsdorfer, L. Ungur, Y. Guo, J. Tang, H.-J. Zhang, L. F. Chibotaru and A. K. Powell, *J. Am. Chem. Soc.*, 2011, **133**, 11948; (g) Y.-N. Guo, G.-F. Xu, P. Gamez, L. Zhao, S.-Y. Lin, R. Deng, J. Tang and H.-J. Zhang, *J. Am. Chem. Soc.*, 2010, **132**, 8538; (h) P. Zhang, Y.-N. Guo and J. Tang, *Coordin. Chem. Rev.*, 2013, **257**, 1728; (i) J. D. Rinehart and J. R. Long, *Chem. Sci.*, 2011, **2**, 2078; (j) J. W. Sharples, Y.-Z. Zheng, F. Tuna, E. J. L. McInnes and D. Collison, *Chem. Commun.*, 2011, **47**, 7650.
- 7 J. Tang, I. Hewitt, N. T. Madhu, G. Chastanet, W. Wernsdorfer, C. E. Anson, C. Benelli, R. Sessoli and A. K. Powell, *Angew. Chem. Int. Ed.*, 2006, **45**, 1729.
- 8 (a) K. R. Meihaus and J. R. Long, *J. Am. Chem. Soc.*, 2013, **135**, 17952; (b) S.-D. Jiang, B.-W. Wang, H.-L. Sun, Z.-M. Wang and S. Gao, *J. Am. Chem. Soc.*, 2011, **133**, 4730; (c) T. T. da Cunha, J. Jung, M.-E. Boulon, G. Campo, F. Pointillart, C. L. M. Pereira, B. Le Guennic, O. Cador, K. Bernot, F. Pineider, S. Golhen and L. Ouahab, *J. Am. Chem. Soc.*, 2013, **135**, 16332; (d) J.-L. Liu, Y.-C. Chen, Y.-Z. Zheng, W.-Q. Lin, L. Ungur, W. Wernsdorfer, L. F. Chibotaru and M.-L. Tong, *Chem. Sci.*, 2013, **4**, 3310; (e) S. D. Jiang, B. W. Wang, G. Su, Z. M. Wang and S. Gao, *Angew. Chem. Int. Ed.*, 2010, **49**, 7448; (f) M.-E. Boulon, G. Cucinotta, J. Luzon, C. Degl'Innocenti, M. Perfetti, K. Bernot, C. Calvez, A. Caneschi and R. Sessoli, *Angew. Chem. Int. Ed.*, 2013, **52**, 350; (g) R. J. Blagg, C. A. Muryn, E. J. L. McInnes, F. Tuna and R. E. P. Winpenny, *Angew. Chem. Int. Ed.*, 2011, **50**, 6530; (h) A. J. Brown, D. Pinkowicz, M. R. Saber and K. R. Dunbar, *Angew. Chem. Int. Ed.*, 2015, **54**, 5864; (i) S. Cardona-Serra, J. M. Clemente-Juan, E. Coronado, A. Gaita-Ariño, A. Camón, M. Evangelisti, F. Luis, M. J. Martínez-Pérez and J. Sesé, *J. Am. Chem. Soc.*, 2012, **134**, 14982.
- 9 (a) L. Ungur, S.-Y. Lin, J. Tang and L. F. Chibotaru, *Chem. Soc. Rev.*, 2014, **43**, 6894; (b) S.-Y. Lin, Y.-N. Guo, Y. Guo, L. Zhao, P. Zhang, H. Ke and J. Tang, *Chem. Commun.*, 2012, **48**, 6924; (c) I. J. Hewitt, J. Tang, N. T. Madhu, C. E. Anson, Y. Lan, J. Luzon, M. Etienne, R. Sessoli and A. K. Powell, *Angew. Chem. Int. Ed.*, 2010, **49**, 6352; (d) B. Hussain, D. Savard, T. J. Burchell, W. Wernsdorfer and M. Murugesu, *Chem. Commun.*, 2009, 1100.
- 10 (a) H. Ke, L. Zhao, Y. Guo and J. Tang, *Eur. J. Inorg. Chem.*, 2011, **2011**, 4153; (b) S.-Y. Lin, L. Zhao, Y.-N. Guo, P. Zhang, Y. Guo and J. Tang, *Inorg. Chem.*, 2012, **51**, 10522; (c) S. Xue, X.-H. Chen, L. Zhao, Y.-N. Guo and J. Tang, *Inorg. Chem.*, 2012, **51**, 13264; (d) L. Zhang, P. Zhang, L. Zhao, J. Wu, M. Guo and J. Tang, *Inorg. Chem.*, 2015, **54**, 5571; (e) S.-Y. Lin, W. Wernsdorfer, L. Ungur, A. K. Powell, Y.-N. Guo, J. Tang, L. Zhao, L. F. Chibotaru and H.-J. Zhang, *Angew. Chem. Int. Ed.*, 2012, **51**, 12767.
- 11 Y.-N. Guo, G.-F. Xu, Y. Guo and J. Tang, *Dalton Trans.*, 2011, **40**, 9953.
- 12 K. R. Meihaus, S. G. Minasian, W. W. Lukens, S. A. Kozimor, D. K. Shuh, T. Tyliczszak and J. R. Long, *J. Am. Chem. Soc.*, 2014, **136**, 6056.

## Graphic abstract

Coupling  $\text{Dy}_3$  triangles results in two unique  $\text{Dy}_6$  complexes showing single-molecule magnetic behaviour with high energy barriers of 116 and 181 K for  $\text{Dy}_6\text{-NO}_3$  and  $\text{Dy}_6\text{-SCN}$ , respectively.

